energy&fuels

Open Access

pubs.acs.org/EF

Article

Structural Changes of Lignin during OrganoCat Processing

Leonie Schoofs, Björn Thiele, Josia Tonn, Tim Langletz, Sonja Herres-Pawlis, Andreas Jupke, Philipp M. Grande,* and Holger Klose*

Cite This: *Energy Fuels* 2024, 38, 4192−4202

Read Online

ACCESS | Metrics & More | Article Recommendations | Supporting Information

ABSTRACT: The isolation of high-quality lignin from lignocellulose plays a pivotal role in the holistic use of biomass. Hence, modern approaches aim to avoid recondensation reactions of lignin during extraction and aim to maintain most of the native structure. This increases its solubility and the proportion of cleavable beta aryl linkages, which can be of advantage in the subsequent process chain. As the lignin structure varies greatly between different plant groups, understanding the effect of lignin structural features on processing and vice versa is a prerequisite for industrial application. In this study, a two-step process using concentrated phosphoric acid in a swelling step and then a biphasic fractionation process utilizing diluted phosphoric acid under mild conditions was used as a benchmark to extract lignin from 10 structurally and compositionally different plant materials. Pyrolysis-gas chromatography−mass spectrometry and $^{1}H-^{13}C$-heteronuclear single quantum correlation-nuclear magnetic resonance were used to identify the monomer unit composition and the linkage proportion of lignin before and after extraction and combined with size exclusion chromatography, wet chemical analysis of the biomass, and fractionation yields to identify correlations before and after processing. After processing, the relative beta aryl ether linkage content decreased greatly from 40−90 to 20−40 linkages per 100 monomer units. The molecular weight (M_w) of extracted lignin was measured to be between 2000 and 6800 Da, indicating that the fractionation process produces relatively uniform lignin in these aspects from different plant sources. Nevertheless, lignin structure properties such as beta aryl and resinol linkages showed an influence on delignification and lignin size.

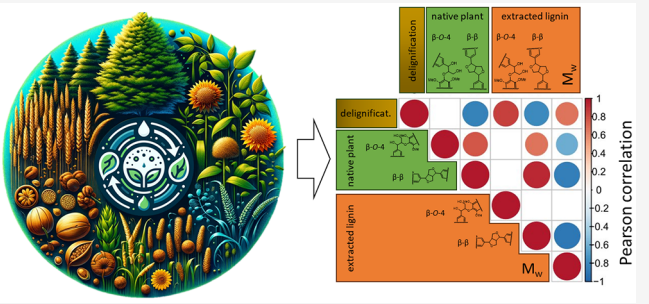

INTRODUCTION

Lignin is, along with structural polysaccharides like cellulose and hemicellulose as the main building blocks of plant cell walls, one of the most common renewable organic structures on earth. It contributes up to 30 wt % of lignocellulosic biomass, therefore displaying an abundant source of aromatic molecules for materials, chemicals, and fuels.[1−3] Traditionally, industrial applications have focused on polysaccharides (mainly cellulose), and there are existing production chains, especially in the pulp and paper or textile industry. For lignin and lignin-based products the market is increasing, but so far, comparably few industrial applications exist.[4,5] In most refineries, it is simply burned to generate energy. Lignin exhibits high heterogeneity and recalcitrance, which provides challenges for its valorization. The lignin sourced from industrially established pulping processes like the Kraft process is highly condensed and can contain sulfur, depending on the process used.[6] Therefore, they are unsuitable for many applications. In recent years, numerous process developments have been made using milder process conditions for biomass fractionation, which can extract lignin with fewer condensation reactions.[7−9] The extraction and provision of lignin that maintains many of its natural functional groups can be of advantage as it is often more soluble, and the higher proportion of accessible ether linkages provides a greater potential for chemical modification.[10,11]

Lignin itself is a macromolecule consisting of phenylpropane derivate subunits. It is synthesized within plants primarily from three canonical 4-hydroxyphenylpropanoids. These monolignols differ in their degree of methoxylation of the aromatic ring. Namely, the three main monolignols are sinapyl alcohol, coniferyl alcohol, and *p*-coumaryl alcohol, which are usually referred to as syringyl (S), guaiacyl (G), and *p*-hydroxyphenyl (H) units. Their polymerization occurs in a combinatorial radical coupling process and produces a series of substructures with a small variety of interunit linkages. Coupling occurs either via ether bonds like the *β*-O-4 (*β*-aryl ether) linkage or as C−C coupling like in the *β*-*β* (resinol) and *β*-5 (phenylcoumaran) motif. The *β*-O-4 coupling is the most prevalent interunit link, comprising, e.g., 50−65% of total linkages in native hardwood lignin.[12] As lignin polymerization

Received: September 24, 2023
Revised: January 30, 2024
Accepted: February 5, 2024
Published: February 22, 2024

is a combinational radical process, the polymer lacks any regular repeating units, making it challenging to characterize and valorize.[13] Depending on the plant species, tissue, developmental stages, and biotic or abiotic factors, lignin can significantly differ in its structure and composition. But the structure is important for lignin valorization, as polymer length and linearity change material properties such as viscosity and crystallinity. Lignin with a high S monomer ratio is known to be more linear, as the additional methoxy group of the syringyl unit protects the cross-linking site on the aromatic ring.[14] β-5 linkages are only possible with guaiacyl monomers and therefore less common in low G lignin.[15] In recent years, several technologies have been developed to emphasize the utilization of lignin. Most of them aim to holistically valorize lignocellulose in biorefineries. The mode of extraction heavily affects lignin chemistry and therefore the application options, not only as replacers for currently petroleum-based commodities but also as novel compounds with new functionalities. In this context, organosolv pretreatments represent very promising strategies because they can be used to extract lignin under comparably mild conditions. The combination of an organic solvent with acids and/or water enables an efficient fractionation of lignocellulose into its three major constituents, an aqueous polysaccharides-derived stream, lignin (precipitate), and a solid residue enriched in cellulose.[5,16] The process used in this study (OrganoCat) utilizes a biphasic, acid-catalyzed approach to fractionate lignocellulosic biomass. At 125−160 °C, the amorphous, noncellulosic sugars become mildly hydrolyzed by a diluted acid within the aqueous phase. A second organic phase of 2-methyltetrahydrofuran (2-MTHF) is used to extract lignin in situ. The different process streams can be separated, and water, solvent, and catalyst can be recycled.[17−19] The comparably mild conditions result in lignins, which maintain many of the native structural features and functional groups.[17]

As described above, the chemical structure of extracted lignin is determined by its source but is also strongly affected by the chemical alterations during the extraction process. We have determined generic chemotypic factors of plant biomass which can influence yield, monomer ratio, and linkage proportion of the produced lignin by single-stage OrganoCat fractionation.[20] Recently, we disclosed an integrated two-step OrganoCat process that utilizes phosphoric acid in concentrated form as an additional swelling step for lignocellulose, followed by a diluted acid pretreatment step. The swelling step enables enhanced extraction yields while retaining a higher proportion of β-O-4 linkages in the organic extract, compared to our previous OrganoCat approaches.[18,19] In this conceptual work with beech wood material, we found that the H/G/S ratio was slightly altered during the extraction process, showing an increased proportion of H-units in the extracted lignin. Furthermore, the number of β-O-4 linkages was reduced to approximately half of the amount initially determined in beech wood, which was significantly lower reduction when compared to the one-step OrganoCat system and other comparable fractionation systems.[17]

Building on these studies, this work aims to explore the lignin extraction during a two-step fractionation using a set of chemotypically different lignocellulosic materials to investigate which original structural features affect the quantity and quality of the extracted lignin, depending on variable plant materials with different chemotypes. As future biorefineries profit from being able to work with different feedstocks, predicting the yield and quality of the lignin depending on the source material's qualitative characteristics will be important to be able to provide specialized products.

MATERIALS AND METHODS

All chemicals were purchased from Carl Roth and Sigma-Aldrich (Germany) and used without further purification.

Plant Biomass Material. The plant biomasses used in this work are from the same set published earlier.[20] In addition, walnut shells were purchased from LEMBERONA GmbH, Austria. A characterization of the plant materials chemotype is available in the Supporting Information (see Supporting Information, Table S1). For maize, the whole plant, including stover and cobbs, was used.

Plant materials were obtained as already dried material and were milled with a cutting mill (SM 200 (Retsch, Haan, Germany) with a 1 mm sieve. Walnut shells were already milled to a fine powder by the manufacturer. These materials were used directly for the OrganoCat pretreatment and fractionation. In preparation of the wet chemical analysis, all materials were additionally ground to a fine powder using a ball mill M 400 (Retsch, Haan, Germany) in a 50 mL metal beaker (30 s^{-1}, 2 min).

Lignocellulose Compositional Analysis. Previously described protocols were used for the wet chemistry-based analysis of lignocellulose with minor adaptations.[21] In brief, alcohol-soluble components were removed, and all analysis was carried out on the residues (AIR). Starch was digested enzymatically to obtain the destarched lignocellulose sample (dAIR) of all materials. Lignin was determined as acetyl bromide soluble lignin (ABSL) and crystalline cellulose content was measured by the Updegraff method, as both were described by Foster et al.[22,23] Noncellulosic polysaccharide composition in dAIR was determined after hydrolysis with trifluoracetic acid (TFA) followed by high-performance anion-exchange chromatography with pulsed amperometric detection (HPAEC-PAD) as described in Damm et al.[24] The total acetate content of the sample was determined using an acetic acid kit (KACE-TRM, Megazyme, Wicklow, Ireland).

Phosphoric Acid OrganoCat Treatment. For the swelling step, 500 mg of plant biomass were mixed with 250 μL of phosphoric acid (85%) and 250 μL of ultrapure water and heated in a closed 25 mL high-pressure reactor at 80 °C for 1 h. The reactor was then cooled and opened. For the fractionation step, 4.5 mL of ultrapure water and 5 mL of 2-MTHF were added to the mixture in the reactor. Ten bar of argon pressure was added to the closed stainless-steel high-pressure reactor with a Teflon inlet to minimize 2-MTHF evaporation. The reactor was heated to 140 °C for 3 h under continuous stirring of the mixture. After cooling and depressurizing, the liquid phase was separated by short centrifugation for 2 min at 1880*g*, and the organic phase was removed with a pipet. To obtain the lignin, the 2-MTHF was evaporated and dried completely in an exicator for 3 days at room temperature. Lignin yield was determined gravimetrically. The aqueous phase was filtered to remove the cellulose-enriched pulp. Sugar concentration and composition were determined from the aqueous phase by HPAEC-PAD. The pulp was dried for 48 h at 80 °C, and biomass mass loss was determined gravimetrically. All lignocellulose fractionations were performed in a minimum of triplets.

2D-NMR Analysis. Both extracted lignin and full biomass were analyzed by $^{1}H-^{13}C$ heteronuclear single quantum correlation nuclear magnetic resonance ($^{1}H-^{13}C$-HSQC-NMR). The biomass was prepared according to the protocol of Cheng et al.[25] using the following optimized conditions. The plant material (1 g) was ground by a Retsch PM 100 planetary ball mill utilizing a 50 mL zirconium dioxide (ZrO_2) vessel containing ZrO_2 ball bearings (10 mm × 10) spinning at 600 rpm with alternating grinding (5 min) and interval breaks (5 min) in a total time of 7 h. Twenty-five mg of biomass were then suspended in 0.75 mL of deuterated dimethylsulfoxide (DMSO-d_6), and 10 μL of 1-ethyl-3-methylimidazolium acetate ([Emim]OAc) was added. The mixture was stirred for 2 h at 60 °C until the biomass dissolved. $^{1}H-^{13}C$-HSQC NMR measurements were taken on a Bruker AVANCE 600 MHz NMR spectrometer with the Bruker

https://doi.org/10.1021/acs.energyfuels.3c03673
Energy Fuels 2024, 38, 4192−4202

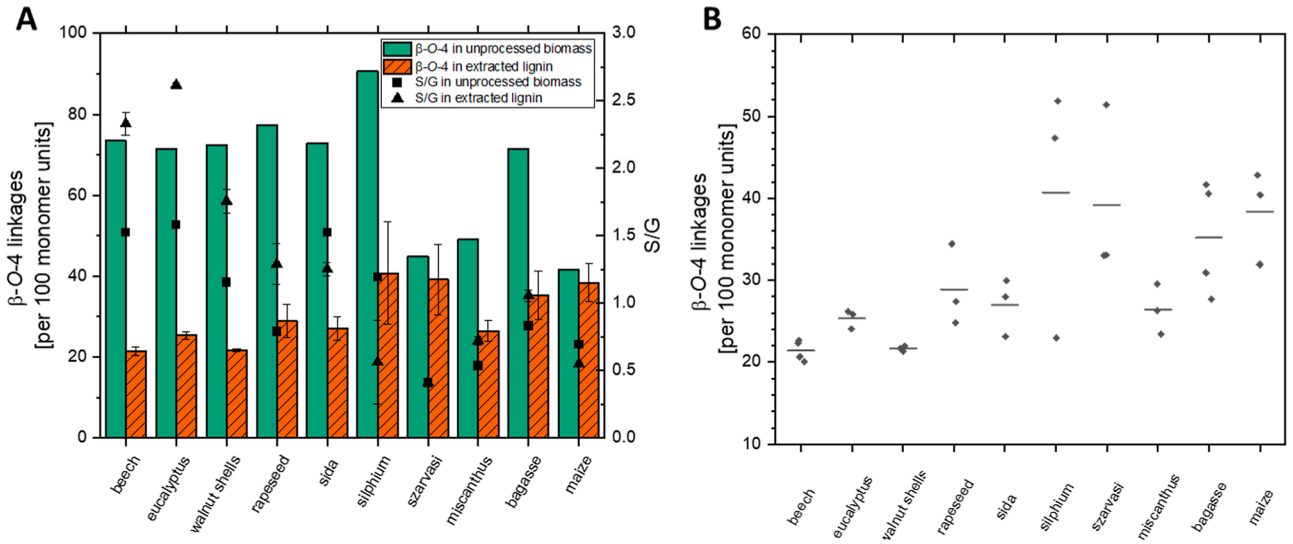

Figure 1. (A) S/G ratio in lignin of unprocessed biomass (single measurement) and S/G ratio of extracted lignin (average of three experiments; in the case of beech and bagasse, average of four experiments) measured by $^{1}H^{13}C$-HSQC-NMR (B) β-O-4 linkage proportion per 100 total S and G units of extracted lignin (average of three experiments; in the case of beech and bagasse, average of four experiments) measured by $^{1}H^{13}C$-HSQC-NMR. For full data set, see Supporting Information, Tables S3 and S4.

standard pulse sequence "hsqcetgpsisp.2". The measurement was conducted with a spectral width of 16 ppm in the F2 (^{1}H) dimension with 2048 data points (TD1) and 240 ppm in the F1 (^{13}C) dimension with 256 data points (TD2), a scan number (SN) of 128, an interscan delay (D1) of 1 s, and an acquisition time of 10 h. The chemical shift was referenced to the solvent DMSO signal ($\delta(^{1}H)$ = 2.500 ppm; $\delta(^{13}C)$ = 39.52 ppm). The signals of monomer units and linkages were integrated and referenced to the lignocellulose structures, according to literature.[25] The sum of aromatic units was calculated using the following formula

$$\Sigma(\text{arom.}) = (S_{2,6}/2 + G_2) + (H_{2,6}/2)$$

The percentage of each unit was calculated as

$$S = (S_{2,6}/2)/\Sigma(\text{arom.}) \times 100\%$$

$$G = (G_2/\Sigma(\text{arom.}) \times 100\%$$

$$H = (H_{2,6}/2)/\Sigma(\text{arom.}) \times 100\%$$

Linkages are given as linkage per 100 monomer units. Due to overlapping peaks, β-O-4 is calculated using only the α proton signal. β-β and β-5 linkages are calculated using all signals of the corresponding linkage. Linkages were calculated according to the following formulas

$$\beta\text{-O-4 linkages} = \alpha\beta\text{-O-4}/\Sigma(\text{arom.}) \times 100\%$$

$$\beta\text{-}\beta \text{ linkages} = (\alpha\beta\text{-}\beta + \beta\beta\text{-}\beta + \gamma\beta\text{-}\beta)/\Sigma(\text{arom.}) \times 100\%$$

$$\beta\text{-5 linkages} = (\alpha\beta\text{-5} + \beta\beta\text{-5} + \gamma\beta\text{-5})/\Sigma(\text{arom.}) \times 100\%$$

Pyrolysis-Gas Chromatography–Mass Spectrometry Analysis. Pyrolysis of lignin samples was performed with a Curie point pyrolizer (Pilodist, Bonn, Germany) coupled to a GC–MS system consisting of a gas chromatograph 7890 and a single quadrupole mass spectrometer 5975C TAD inert XL MSD (Agilent, Santa Clara, CA, USA). 1–2 mg of powdered biomass or pulp samples were filled into tubes (0.9 cm length, 1.8 mm i.d.) self-made from ferromagnetic metal foils (nickel–iron alloy, 0.9 × 0.67 cm, Japan Analytical Industry, T_C = 590 °C). The metal tube was sealed by pressing with flat pliers, inserted in a glass liner, and placed in the pyrolizer. Pyrolysis was carried out in a glass liner at 590 °C for 10 s. Lignin pyrolysis products were separated on an Optima-5-HT column (60 m × 0.25 mm inner diameter, 0.25 μm film thickness, Macherey-Nagel, Germany). Helium was used as the carrier gas at a constant gas flow of 1.0 mL/min. The GC oven was programmed from 80 to 340 °C (held for 20 min) at a rate of 5 °C/min. The injector temperature was held at 280 °C, and all pyrolysis was conducted in split mode (1:10). The mass spectrometer was used in electron impact (EI, 70 eV) mode and scanned over the range m/z 30–650. The GC interface and ion chamber were kept at 280 and 250 °C, respectively. A self-made C8–C24 alkane mixture solution was analyzed for better assignment of the peaks in the pyrolysis chromatograms by calculation of their Kovaťs indices. Data processing was performed by using MassHunter 4.2 (Agilent, Santa Clara, Ca, USA). The pyrolysis products were identified by comparison of their mass spectra with those in the NIST and Wiley mass spectral libraries, by comparison with compounds reported in the literature,[26] and by their Kovaťs indices.

SEC Measurements. The organic extract was solved in 0.5 mL of acetone and precipitated in 30 mL of cold water. The solid was separated by centrifugation, washed with 2 × 25 mL H_2O, and dried again.

The distribution of molecular sizes in the lignin samples was examined through size exclusion chromatography (SEC). The analysis was carried out using an Agilent Series 1200 SEC device featuring an RID detector (Optilab Rex 837, Wyatt Technology) and a SEC column system comprising a precolumn PSS PolarSil (8 × 50 mm, 5 μm particle size) and three columns of PSS PolarSil Linear S (8 × 300 mm, 5 μm particle size) in series. The SEC measurements utilized *N*,*N*-dimethylformamide with 0.1 M lithium chloride as the eluent, maintained at a column temperature of 45 °C and a flow rate of 1 mL min^{-1}. Lignin samples at a concentration of 30 g L^{-1} were dissolved in the eluent, with an injection volume of 10 μL. Calibration was performed using the PSS ReadyCal-Kit Poly(styrene) standard, covering a molecular weight range from 266 to 66,000 Da, and the eluent matched that of the lignin samples. PSS WinGPC software was employed for the analysis of the SEC data.

Statistical Analysis. Pearson correlations P (significance of $p < 0.05$) were made between various parameters of native and extracted biomass and results of lignin analytics. Normality was not assumed. To assess the significance of differences between the extract yields and lignin characteristics, variance analysis for nonparametric data (Kruskal–Wallis test, $p < 0.05$) was performed. The statistical analyses were made by SPSS IBM Statistics v25.0 (2017).

Delignification. Delignification was calculated as the relative removal of lignin from the solid residue measured by the AcBr method.

https://doi.org/10.1021/acs.energyfuels.3c03673
Energy Fuels 2024, 38, 4192–4202

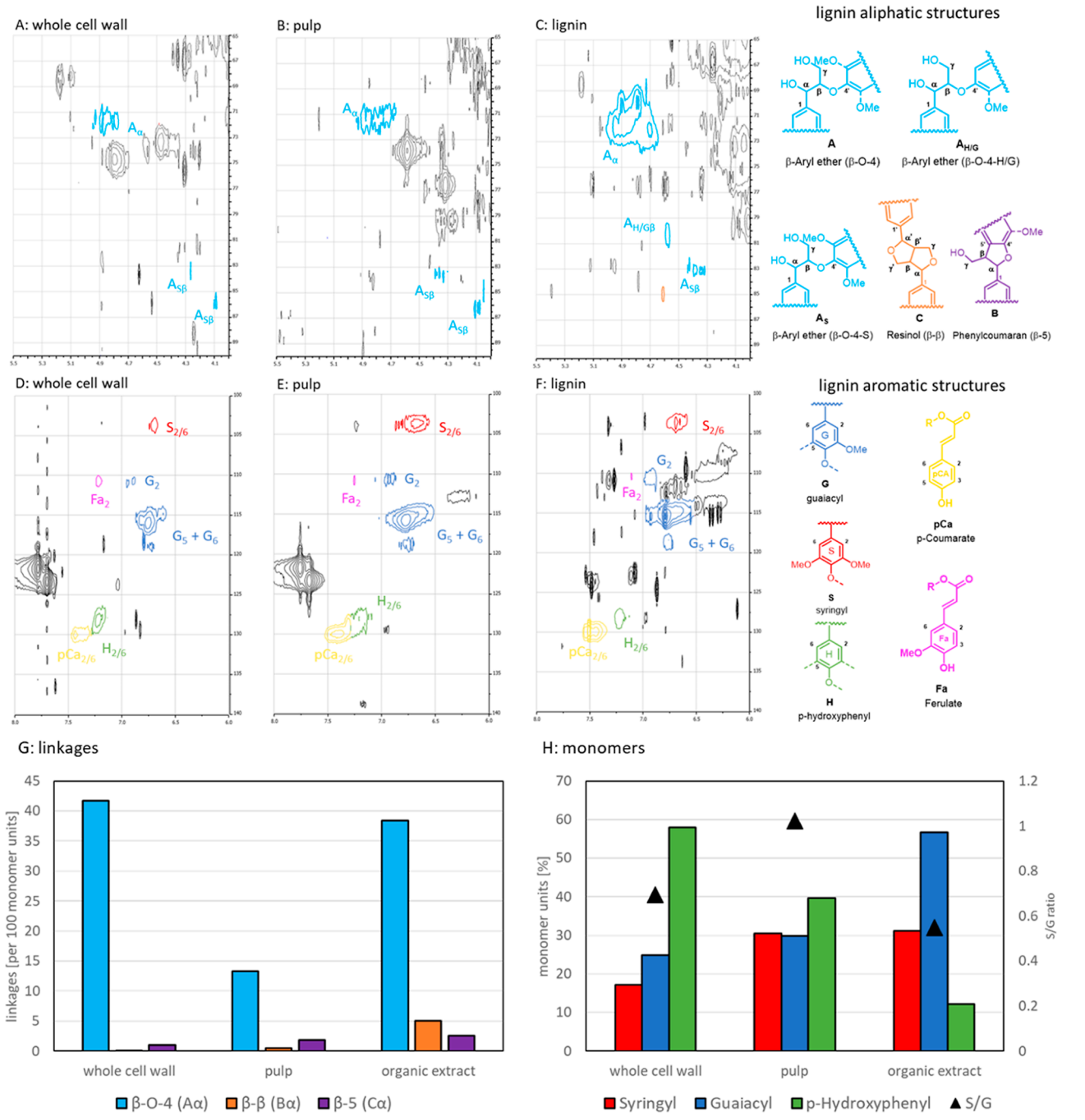

Figure 2. Partial 2D HSQC-NMR spectra of whole cell wall (A,D), pulp (B,E), and lignin after OrganoCat extraction (C,F) of maize. The top three spectra: relevant lignin aliphatic region (δ_H = 4.0−5.5 ppm, δ_C = 65−90 ppm). The bottom three spectra: lignin aromatic region (δ_H = 6.0−8.0 ppm, δ_C = 100−140 ppm). (G) Lignin linkage proportion per 100 monomer units determined by HSQC-NMR integrals of β-aryl ether (Aα), phenylcoumaran (Bα), and resinol (Cα). (H) Relative monomer composition determined by HSCQ-NMR integrals of syringyl (S2/6), guaiacyl (G2), and *p*-hydroxyphenyl (H2/6).

$$\text{Delignification} = \left(1 - \frac{\text{AcBr lignin in pulp}\cdot\text{pulp yield}}{\text{AcBr lignin in unprocessed plant}}\right)\%$$

RESULTS AND DISCUSSION

We used a comprehensive set of analytical techniques to characterize the chemical changes in the lignin from ten chemotypically different plant biomasses due to extraction. Key factors analyzed to determine the lignin structure are the monomer composition and the proportion of β-O-4 linkages before and after extraction.[27]

Structural Changes of Lignin during Processing. Analysis of the selected plants showed a wide proportional range of β-O-4 linkages from 40 to 90 linkages per 100 S and G units in the untreated biomass (Figure 1A). While beech, eucalyptus, walnut shells, sida, silphium, and sugar cane bagasse all contain a high proportion of β-O-4 linkages (70−90 linkages per 100 S and G units), the grasses szarvasi, miscanthus, and maize have far fewer ether linkages (40−50

https://doi.org/10.1021/acs.energyfuels.3c03673
Energy Fuels 2024, 38, 4192−4202

linkages per 100 S and G units). During the extraction process, some of the β-O-4 linkages get cleaved. We did not find any correlation between the β-O-4 linkages in the extracted lignin and the β-O-4 linkages in the untreated biomass (see Supporting Information, Table S5). Thus, we assume that factors other than the original bond proportion mainly determine the proportion of residual bonds after extraction. While statistical analysis (Kruskal−Wallis) of the whole data set showed a significant difference in β-O-4 linkages between all extracted lignins ($p < 0.05$), the posthoc pairwise comparison did not reveal a single pair in which the β-O-4 linkages were statistically different (Figure 1B). This indicates that the extraction leads to a homogeneous distribution of β-O-4 linkage proportions in the extracted lignin, independent of the original proportion in the different untreated biomasses.

In our previous studies, we already observed that the β-O-4 linkages in the residual lignin of the cellulose-enriched solid residue of beech wood derived from the PA OrganoCat process were reduced from 73 to 21 linkages per 100 monomer units, while 38 linkages per 100 monomer units were left in the extracted lignin. We observed similar results for maize (Figure 2).

Although the relative reduction of β-O-4 linkages between the native maize biomass and the extracted lignin is smaller than the one observed for beechwood processing (Figure 2G), the residual lignin in the pulp exhibited a reduction in β-O-4 linkages to approximately 1/3 of the untreated biomass. This indicates that the ether linkages are mostly cleaved by the acid within the lignocellulose. When the lignin is sufficiently disentangled, it can be extracted into the 2-MTHF phase, where only small amounts of acid catalyst are present, and therefore, further cleavage or recondensation of the lignin fragments is reduced. A certain proportion of β-O-4 linkages or a related range of molecular size might also be easier to extract and dissolve in the organic solvent, which would lead to a relatively similar level of ether linkages in the extracted lignins across the different plants.

The S/G ratio of maize lignin increased in pulp, while it decreased in the extracted lignin. In maize, G-rich lignin seems to be favored for extraction. Solvents like DMSO or THF with medium polarity are known to solubilize lignin well.[28] The models of Petridis et al. show that the solvent−lignin interaction is independent of lignin monomer composition in the case of THF/water,[29] while Beckham et al.[28] suggest high G content to be favorable for the extraction. Branching and size of the lignin may have a larger influence on lignin solvability than monomer composition. 2-MTHF, which is used in the OrganoCat process, has a miscibility gap with water, leading to a biphasic system. The lignin extraction mechanism and potential reactions after extraction are therefore likely to differ from those of THF/water mixtures. After the OrganoCat process, lignin from different plant sources possesses similar β-O-4 linkage proportion and solubility in 2-MTHF. This enhanced uniformity of OrganoCat lignins might be advantageous in future refinement processes, as processing usually involves solubilization of the material.

Induced Changes in Lignin Composition. The S/G ratio was measured by HSQC-NMR and Py-GC-MS before and after processing (Table 1). The monomer ratio changed between native and extracted lignin. In the HSQC-NMR measurements for beech, eucalyptus, walnut shells, miscanthus, sugar cane bagasse, and rapeseed, the S/G ratio increased after processing, while it decreased for sida and maize. For szarvasi, no change in the S/G ratio was observed. HSQC-NMR of the extracted lignin showed good reproducibility (Table 1).

Table 1. S/G Ratio of Lignin of Selected Plants before Processing and after OrganoCat Extraction[a]

	NMR S/G native	NMR S/G extracted[b]	Py-GC-MS S/G native	Py-GC-Ms S/G extracted
beech	1.53	2.33 (0.08)	1.68	1.35
eucalyptus	1.58	2.62 (0.02)	1.70	1.57
walnut shells	1.15	1.76 (0.09)	1.15	0.96
sida	1.52	1.25 (0.05)	1.00	0.79
silphium	1.20	0.56 (0.31)	0.91	0.71
szarvasi	0.41	0.41 (0.02)	0.38	0.28
miscanthus	0.54	0.72 (0.03)	0.55	0.53
sugar cane bagasse	0.83	1.06 (0.04)	0.76	0.77
rapeseed	0.79	1.29 (0.15)	0.99	0.90
maize	0.69	0.55 (0.00)	0.48	0.38

[a]Measured by HSQC-NMR and Py-GC-Ms. Triplicates of at least three technical replicates were measured with HSQC-NMR for extracted lignin. Standard deviation in brackets. [b]Averages and standard deviations (brackets), determined by measuring 3 technical replicates.

The change in the lignin S/G ratio between untreated biomass and extracted lignin can have different reasons. While demethoxylation from S to G is technically possible, it is unlikely under the given reaction conditions. An alternative explanation is that extractable lignin under the applied conditions is different from residual, more recalcitrant lignin. However, it remains unclear whether these more accessible parts are predominantly composed of S or G, as this appears to vary among different plant species.

Opposed to S and G units, H units before and after extraction did not match, but H units were considerably higher in the unprocessed biomass. Plant biomass has many components in varying amounts, which can cause overlapping signals in the HSQC-NMR. H units can be overestimated due to the 2/6 signal of *p*-hydroxyphenyl overlapping with the 3/5 correlation peak of phenylalanine, although the expected amount in the whole cell wall is very low. More prominently, the *p*-coumarate signal that is especially found in grasses also presents a possible overlap with the 2/6 signal of H-units, as exemplarily pointed out in the spectra shown in Figure 2D−F.[30−32] Therefore, in the following, the linkages refer to S and G units only.

Comparing different species by their pyrolysis products must be done with caution because samples may vary in the abundance of certain compounds, such as ferulates. These compounds may produce similar pyrolysis products, which can be misassigned to different lignin monomers.[33] The pyrolysis reactions of native biomass and extracted lignin are complex, as the molecular building blocks and their structural organization vary greatly between plants and through processing. Ionization potential and stabilization of certain molecules depend greatly on their surrounding matrix. Additionally, the formation of char during pyrolysis from lignin may slightly alter monomer ratios because char formation might not occur homogeneously.[34] Here, the S/G ratio determined by Py-GC-MS showed a comparable ranking for the 10 biomasses, as observed by HSQC-NMR determination. The observed changes in the S/G ratio during the fractionation process, however, differ from the HSQC-NMR measurements. While

https://doi.org/10.1021/acs.energyfuels.3c03673
Energy Fuels 2024, 38, 4192−4202

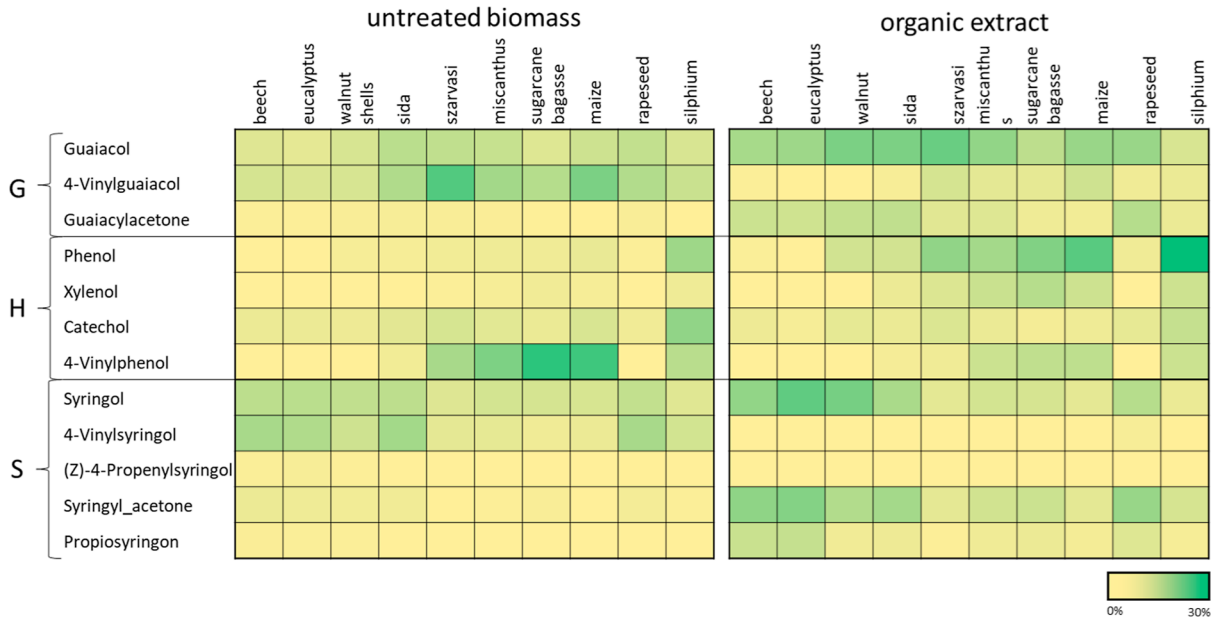

Figure 3. Heatmap showing the relative abundance of selected pyrolysis products detected by Py-GC-MS. Compounds with a difference >5% between the analysis of the whole cell wall and lignin were selected. Color density represents the percentage of the pyrolysis product within the total of all pyrolysis products of the respective plant. For the full data set, see Supporting Information, Table S6.

the S/G ratio determined by Py-GC-MS for beech and eucalyptus decreases in the extracted lignin, it increases when measured by HSCQ-NMR. The observed differences between both methods are consistent with other studies.[32] According to Happs et al., HSQC-NMR is determined to be the most suitable method for comparing the lignin monomer ratio between different species, although it exhibits some limitations.[35] It underestimates the amount of S units, which we can observe in our data, and the S/G ratio measured by Py-GC-MS is higher for most plants except for the S dominant lignin of beech and eucalyptus. Py-GC/MS is rapid and highly sensitive for characterizing the chemical structure of lignin, especially for the estimation of the S/G ratio of lignin.[36−39] However, phenols formed during pyrolysis predominantly result from the cleavage of β-O-4 and β-5 linkages.[40,41] Subsequently, Py-GC/MS overestimates the number of S units in lignin. While both methods have their limitations, they together can give valuable insights and a more comprehensive view into the differences in monomer structure between the selected plants.

Since a standardized evaluation of the pyrolysis products[21] did not yield a clear pattern in the changing monomer ratios before and after treatment, we had a detailed look into the pyrolysis products generated from lignin in untreated biomass and extracted lignin (Figure 3).

The pyrolysis data for untreated material exhibit a higher abundance of the 4-vinyl products from the different S, G, and H than in extracted lignin, which is in accordance with higher levels of β-O-4 linked units in the untreated biomass. Woody biomasses from beech, eucalyptus, walnut shells, and sida especially exhibited 4-vinylsyringol, whereas the grasses, szarvasi, miscanthus, sugar cane bagasse, and maize, exhibited 4-vinylguaiacol and 4-vinylphenol. Lignin interunit linkages as *p*-coumarate and ferulate lead to the formation of the same pyrolysis products, 4-vinylphenol and 4-vinylguaiacol, respectively, which has to be considered in the evaluation of the data.[42] Due to the absence of carbohydrates, a higher abundance of methoxylated and ethoxylated compounds can be observed in the extracted lignins (see Supporting Information, Table S6). Polysaccharides, particularly xylan, can act as hydrogen donors for the elimination of aromatic substituents by replacing them with hydrogen.[43] Generally, the interactions between lignin and polysaccharides at a specific temperature can significantly affect the pyrolysis products.[44]

A comparison of the pyrolysis products with chemical lignin features (AcBr lignin in pulp, AcBr lignin in untreated biomass, and delignification) revealed only a few correlations (Table S8). Especially phenol showed a negative correlation with these factors, whereas syringol and methylsyringol exhibited positive factors. While phenol is a product that is formed after the elimination of aromatic substituents, syringol and methylsyringol still contain their aromatic substitutions.[44] Guaiacols and syringols rapidly transit to catechols and phenols when the pyrolysis temperature is increased to 400−450 °C, and the secondary pyrolysis reactions take place and sufficient H-donors are available.[43] Interestingly, siphium lignin exhibited a remarkably high abundance of catechols and phenols after pyrolysis of the untreated biomass, in contrast to other biomasses, where these products occurred only in the pyrolysis of extracted lignin.

Analysis of the interactions between lignin, carbohydrates, and other constituents in future studies might determine further molecular parameters explaining lignin extraction or retention, respectively.

Molecular Size Distribution of Extracted Lignins. The molecular weight of the lignin extracted using the OrganoCat method was determined using gel permeation chromatography, and the results are presented in Table 2. It is important to note that in SEC, molecules are separated based on their hydrodynamic radius, which can vary depending on the monomer ratios and hydroxy groups present in the lignin. This should be taken into consideration when interpreting the exact molecular sizes of the lignins.

https://doi.org/10.1021/acs.energyfuels.3c03673
Energy Fuels 2024, 38, 4192−4202

Table 2. SEC Chromatography Data for the Weight Average (M_w) and Number Average (M_n) Molecular Mass of Extracted Lignin and Polydispersity Index (PDI)

biomass	M_w [Da]	M_n [Da]	PDI
beech	3595	915	3.9
eucalyptus	3088	781	4.0
walnut shells	3983	881	4.5
sida	4069	637	6.4
silphium	1996	357	5.6
szarvasi	4827	729	6.6
miscanthus	4229	885	4.8
sugar cane bagasse	5953	1298	4.6
rapeseed	3128	166	18.9
maize[a]	6775 (855)	1016 (166)	7.0 (1.8)

[a]For maize the average of three experiments and their corresponding measurements are shown to prove repeatability of results. Standard deviation in brackets.

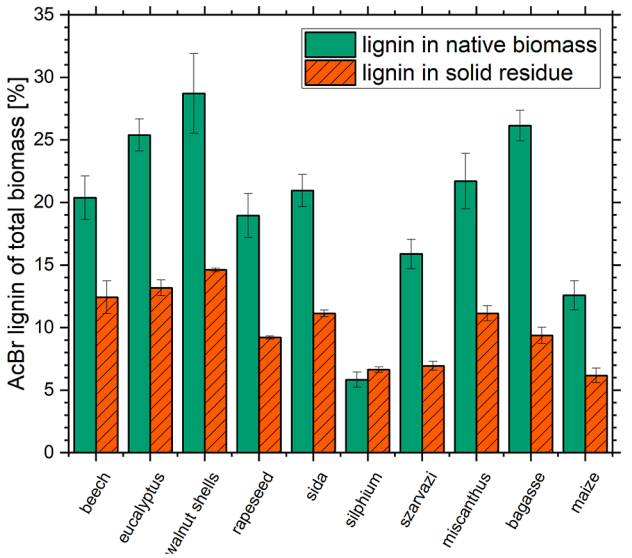

Figure 4. AcBr lignin measured in the unprocessed biomass and AcBr in the pulp after the OrganoCat process (all measurements are in triplicate). Lignin in pulp values were scaled by the corresponding pulp yield to facilitate comparison. All measurements were done in triplicate.

The average determined molecular weight (M_w) of the OrganoCat-extracted lignins varies between 2000 and 7000 Da depending on the species, with most being around 4000 Da. When comparing lignins from the different plant sources, it is worth noting that the extracted wood lignins from beech, eucalyptus, and walnut shells tend to have molecular weights smaller than those of the grass lignins from szarvasi, miscanthus, sugar cane bagasse, and maize. Additionally, the silphium lignin had the smallest average molecular weight, showing three peaks in the SEC chromatogram and suggesting the presence of smaller molecules in the extract that do not necessarily belong to lignin. Maize lignin exhibited the largest average molecular weight, a finding which is supported by the high abundance of β-O-4 linkages in the extracted lignin.

The size distribution in grasses is a bit wider than that in woods. Rapeseed has a very high PDI compared to the lignins from other plants, mainly due to a very low M_n due to the many small molecules in the extract.

Effects of Lignin Structure on Delignification. The delignification efficiency was determined by comparing the amount of lignin content measured in the unprocessed biomass to the residual lignin content in the pulp (Figure 4).

The selected plants vary strongly in lignin content between 6 and 29%. While the amount of lignin in the solid residue also varies between 6 and 14%, we did not observe any linear correlations between the lignin content of the native plant biomass and residual lignin content in the solid residue after OrganoCat. So, a high lignin content in the plant does not necessarily mean that a large amount of lignin is extracted. Beech, walnut shells, and sida have a high initial lignin content but are more recalcitrant toward fractionation as they retain more than half of their lignin (60, 53, and 53%, respectively) in the solid residue. For the grasses szarvazi and bagasse, we measure the lowest residual lignin in pulp relative to the initial plant (35 and 40%, respectively). Consequently, the initial lignin content of the plant does not determine delignification efficiency, underlining that characteristics such as lignin or hemicellulose structure play a role in this fractionation efficiency.

For silphium, the measured lignin in the native biomass is especially low, and the lignin content in pulp was measured to be about the same. Nevertheless, we found a 19% yield of silphium lignin. A detailed look into the composition analysis of silphium shows that the biomass contains 21% alcohol-soluble components (protein and neutral sugars, glycolipids, phospholipids, chlorophyll, triglycerides, pectin) and 35% starch. These values might be slightly overestimated by mass loss of lignocellulose in the destarching process. The high amount of nonlignocellulosic components might influence measurement accuracy for silphium as the lignin in total biomass is given relative to total biomass, including alcohol-soluble components and starch. In the OrganoCat process, we start from the complete biomass, and while we clearly see in the HSQC-NMR that lignin is extracted from silphium, we have to assume that some of the secondary metabolites are also extracted into the 2-MTHF and therefore add to the lignin weight. This is also indicated by other lignin analytics. The SEC chromatogram of extracted silphium lignin showed three peaks, including one around 150 Da, instead of one, as for the other plant extracts (see Supporting Information, Figure S1), and the pyrolysis profile of the untreated silphium biomass exhibited a high abundance of catechols and phenols.

To characterize how structural lignin characteristics in different plants affect the fractionation efficiency, we conducted a Pearson correlation of fractionation yields and structural lignin parameters (Figure 5).

All yield values were calculated relative to the initial biomass weight. After conducting variance analysis with a post hoc pairwise comparison, it was found that there were no significant differences in lignin yield extracted with OrganoCat. However, there were significant differences ($p < 0.05$) in solid residue yield and sugar yield between the plants. Notably, a high solid residue yield indicates a lower extraction of hemicellulose and lignin. Eucalyptus showed the highest amount of solid residue with 60% of the biomass. The solid residues of beech, walnut shells, sida, miscanthus, bagasse, and rapeseed were around 50%, while szarvasi, silphium, and maize solid residues were less than 40% of the original biomass. Eucalyptus, silphium, and miscanthus yielded a lower amount of sugar (15−20 wt %). Beech, walnut shells, sida, szarvasi, sugar cane bagasse, and rapeseed yield a medium amount of sugar (25−35 wt %), and maize resulted in very high sugar

https://doi.org/10.1021/acs.energyfuels.3c03673
Energy Fuels 2024, 38, 4192−4202

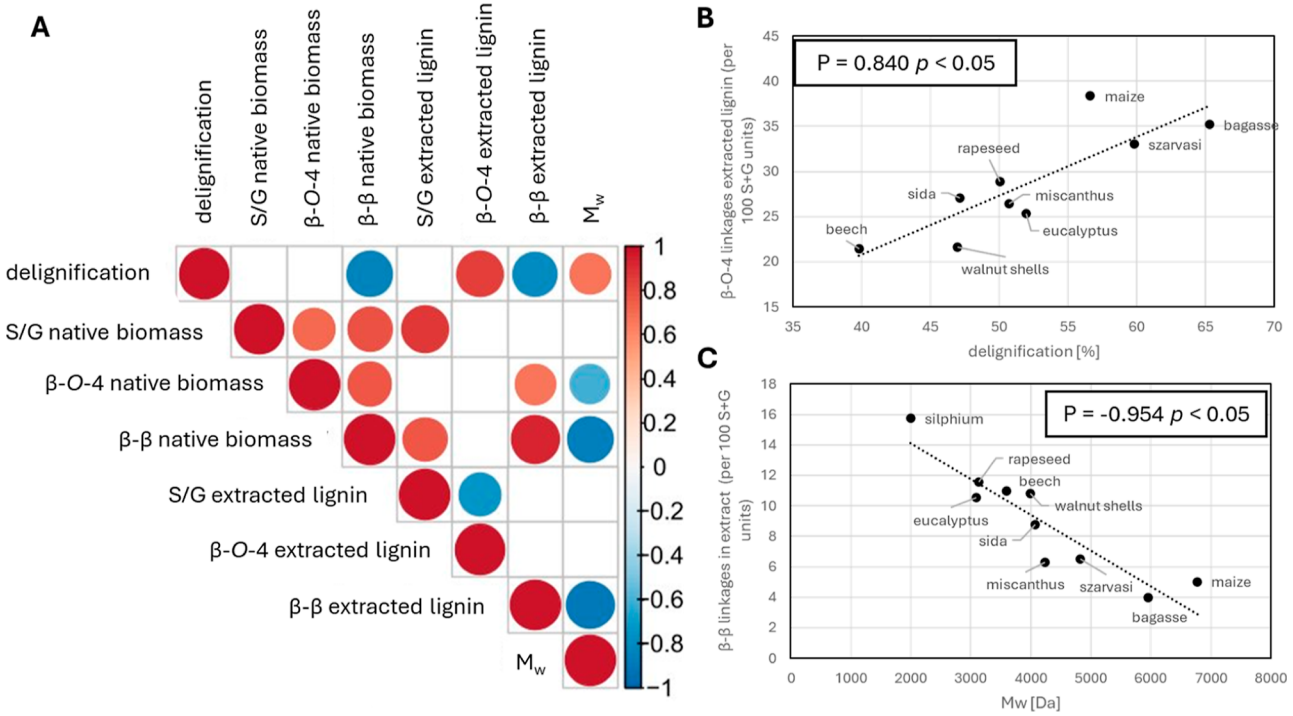

Figure 5. (A) Schematic illustration of Pearson coefficients between delignification and characterization of the native and extracted lignin (β-O-4 linkages, β-β linkages, S/G ratio, M_w). (B) Correlation between β-O-4 linkages proportions was determined by $^{1}H^{13}C$-HSQC-NMR of extracted lignin and delignification. (C) Correlation between β-β linkages in native biomass determined by $^{1}H-^{13}C$-HSQC-NMR and weight average molecular mass M_w determined by SEC. For detailed Pearson coefficients, see Supporting Information, Table S5.

yields with a large variation (65 ± 17 wt %). Since the whole plant including the cob was used, the high sugar yields of maize are caused by a large amount of accessible starch, which is hydrolyzed during the process and adds to the sugar yield with a high proportion of glucose (see Supporting Information, Table S2). Even though we could not find any direct correlation between the yield of hemicellulose sugars and delignification, fractionation efficiency, and lignin properties, it is known that hemicelluloses do have interlinkages with lignin (lignin carbohydrate complexes) and play a complex role in biomass fractionation.[45]

The amount of solid residue does not correlate with the amount of sugar or crystalline cellulose in the unprocessed biomass; however, the amounts of starch (P = 0.768) and alcohol-soluble residues (P = 0.941) show significant (p < 0.05), positive correlations. The alcohol-soluble residues can be extracted into the organic phase, and the starch is depolymerized to glucose, which can be found in the sugar hydrolysate fraction after processing. The amount of solid residue also correlates with the proportion of lignin in the unprocessed biomass (P = 0.814, p < 0.05), confirming the influence of lignin on lignocellulose recalcitrance.[20]

The delignification of the biomass correlates negatively with the β-β linkage proportion in native (P = −826, p < 0.05) and extracted (P = −791, p < 0.05) lignin, meaning that in plants with more β-β linkages in lignin, the relative amount of lignin removed from the solid is smaller. We find a positive correlation with delignification for β-O-4 linkages of the extracted lignin (P = 0.840, p < 0.05) and M_w (P = 0.746, p < 0.05). This means that in plants with lower recalcitrance toward delignification, the extracted lignin is larger and has more ether linkages remaining. The grasses, maize, szarvasi, and bagasse, showed high delignification and a high proportion of β-O-4 linkages in the extracted lignin, hinting that their lignin is more easily accessible for extraction. The woody species, beech, eucalyptus, and the walnut shells show lower delignification and a lower proportion of β-O-4 linkages. As in our other results, sida showed similar behavior to the woody biomasses. Interestingly, rapeseed and miscanthus behave more similarly to eucalyptus and sida than to the other grasses, showing midrange delignification and ether linkages in the extract. Silphium was not considered for delignification, as interferences in the lignin determination resulted in higher lignin measured in pulp than in the original biomass (see Figure 4).

While the native β-O-4 linkage proportion does not correlate with the β-O-4 linkages in the extracted lignin, it shows a weak negative correlation with M_w of the extracted lignin (P = −0.683, p < 0.05). The M_w also correlates negatively with the β-β linkages of native (P = −0.738, p < 0.05) and extracted lignin (P = −0.954, p < 0.05). This means that a large proportion of β-ether and resinol structures per 100 monomer units leads to smaller extracted lignin molecules. This is in accordance with resinol linkages being difficult to break in the process and therefore providing recalcitrance within the biomass. As it is known that resinol linkages occur a lot at the starting points of lignin chains, the lignins with high β-O-4 and β-β linkage amount probably have more chains, thus leading to smaller molecules when ether linkages are cleaved.[30]

While the β-β linkage proportion and molar mass average in the extract correlate, they only slightly cluster in our previously defined plant groups. The grasses, miscanthus, szarvasi, sugar cane, and maize, have a small number of β-β linkages and their extracted lignin has a high molecular weight, while the woody species, beech, eucalyptus, and walnut shells, fall into the higher β-β−lower M_w range. Sida once again proves to be close

https://doi.org/10.1021/acs.energyfuels.3c03673
Energy Fuels 2024, 38, 4192−4202

to the wooden biomasses, while silphium is on the very extreme of small M_w and high β-β. Rapeseed falls out of the categorization, as we expected it to be closer to the grasses, but it turns out to have similar β-β and M_w as the woods.

CONCLUSIONS

Lignocellulose recalcitrance toward fractionation of its main components, cellulose, lignin, and hemicelluloses, is complex and depends on many factors. To understand the influence of biomass features on the phosphoric acid-catalyzed OrganoCat fractionation with a preceding swelling step, the process was applied to 10 chemotypically different plant biomasses. Included in this study were hardwoods, grasses, and agricultural waste products. Special emphasis was placed on lignin and its structure before and after processing, since it is inherently different within these plant types and can play a major role in their recalcitrance. While the lignins of the different untreated plant biomasses showed significant differences in β-O-4 linkage content before the extraction, they were homogenized during the process, showing no significant difference after extraction. A clear reduction of the β-O-4 linkage content was also observed in the pulp, indicating cleavage of larger lignin molecules before the extraction. The 10 different plants also yielded lignins with a similar average weight in the extract. In contrast, the S/G monomer unit ratio stayed in a similar range after processing as in the untreated biomasses. A detailed look into the pyrolysis products from Py-GC-MS showed that internal hydrogenation of aromatic substituents was likely caused by polysaccharides and secondary metabolites acting as internal hydrogen donors. Finally, plants with higher delignification, which were mainly grasses, were shown to retain more β-O-4 linkages in the extracted lignin, suggesting that their lignin is more easily accessible in the applied fractionation process. Resinol linkages in the lignin were found to negatively correlate with molecular weight and delignification, indicating that due to the robustness of β-β linkages, more β-O-4 linkages need to be cleaved to extract lignin, making it more recalcitrant.

ASSOCIATED CONTENT

Supporting Information

The Supporting Information is available free of charge at https://pubs.acs.org/doi/10.1021/acs.energyfuels.3c03673.

Detailed structural data of the biomass composition, fractionation yields, analytical lignin characteristics, and Pearson coefficients (PDF)

AUTHOR INFORMATION

Corresponding Authors

Philipp M. Grande − *Institute for Bio and Geo Sciences 2, Plant Sciences, Forschungszentrum Jülich GmbH, 52428 Jülich, Germany; Bioeconomy Science Center (BioSC), Forschungszentrum Jülich GmbH, 52425 Jülich, Germany;* orcid.org/0000-0002-2137-4920; Email: p.grande@fz-juelich.de

Holger Klose − *Institute for Bio and Geo Sciences 2, Plant Sciences, Forschungszentrum Jülich GmbH, 52428 Jülich, Germany; RWTH Aachen University, 52074 Aachen, Germany; Bioeconomy Science Center (BioSC), Forschungszentrum Jülich GmbH, 52425 Jülich, Germany;* Email: h.klose@fz-juelich.de

Authors

Leonie Schoofs − *Institute for Bio and Geo Sciences 2, Plant Sciences, Forschungszentrum Jülich GmbH, 52428 Jülich, Germany; RWTH Aachen University, 52074 Aachen, Germany*

Björn Thiele − *Institute for Bio and Geo Sciences 2, Plant Sciences, Forschungszentrum Jülich GmbH, 52428 Jülich, Germany; Institute for Bio and Geo Sciences 3, Agrosphere, Forschungszentrum Jülich GmbH, 52428 Jülich, Germany*

Josia Tonn − *AVT-Fluid Process Engineering, RWTH Aachen University, 52074 Aachen, Germany; Bioeconomy Science Center (BioSC), Forschungszentrum Jülich GmbH, 52425 Jülich, Germany*

Tim Langletz − *Institute of Inorganic Chemistry, RWTH Aachen University, 52074 Aachen, Germany; Bioeconomy Science Center (BioSC), Forschungszentrum Jülich GmbH, 52425 Jülich, Germany*

Sonja Herres-Pawlis − *Institute of Inorganic Chemistry, RWTH Aachen University, 52074 Aachen, Germany; Bioeconomy Science Center (BioSC), Forschungszentrum Jülich GmbH, 52425 Jülich, Germany;* orcid.org/0000-0002-4354-4353

Andreas Jupke − *Institute for Bio and Geo Sciences 2, Plant Sciences, Forschungszentrum Jülich GmbH, 52428 Jülich, Germany; AVT-Fluid Process Engineering, RWTH Aachen University, 52074 Aachen, Germany; Bioeconomy Science Center (BioSC), Forschungszentrum Jülich GmbH, 52425 Jülich, Germany;* orcid.org/0000-0001-6551-5695

Complete contact information is available at: https://pubs.acs.org/10.1021/acs.energyfuels.3c03673

Author Contributions

The manuscript was written through contributions of all authors. All authors have given approval to the final version of the manuscript.

Funding

This work was performed as part of the Bioeconomy Science Center (BioSC), supported by the project LignoTex. The scientific activities of the Bioeconomy Science Center were financially supported by the Ministry of Innovation, Science, and Research within the framework of the NRW Strategieprojekt BioSC (no. 313/323-400-00213).

Notes

The authors declare no competing financial interest.

ACKNOWLEDGMENTS

The authors would like to thank Dagmar Drobietz, Vanessa Ploeger, Annika Ruers, and Tom Hübner for contributing to the material preparation and wet chemical analysis of the plant materials.

REFERENCES

(1) Ragauskas, A. J.; Beckham, G. T.; Biddy, M. J.; Chandra, R.; Chen, F.; Davis, M. F.; Davison, B. H.; Dixon, R. A.; Gilna, P.; Keller, M.; Langan, P.; Naskar, A. K.; Saddler, J. N.; Tschaplinski, T. J.; Tuskan, G. A.; Wyman, C. E. Lignin Valorization: Improving Lignin Processing in the Biorefinery. *Science* **2014**, *344* (6185), 1246843.

(2) Lange, H.; Rulli, F.; Crestini, C. Gel Permeation Chromatography in Determining Molecular Weights of Lignins: Critical Aspects Revisited for Improved Utility in the Development of Novel Materials. *ACS Sustain. Chem. Eng.* **2016**, *4* (10), 5167−5180.

(3) Rinaldi, R.; Jastrzebski, R.; Clough, M. T.; Ralph, J.; Kennema, M.; Bruijnincx, P. C. A.; Weckhuysen, B. M. Paving the Way for

Lignin Valorisation: Recent Advances in Bioengineering, Biorefining and Catalysis. *Angew. Chem., Int. Ed.* **2016**, *55* (29), 8164−8215.
(4) Garlapati, V. K.; Chandel, A. K.; Kumar, S. J.; Sharma, S.; Sevda, S.; Ingle, A. P.; Pant, D. Circular Economy Aspects of Lignin: Towards a Lignocellulose Biorefinery. *Renewable Sustainable Energy Rev.* **2020**, *130*, 109977.
(5) Schutyser, W.; Renders, T.; Van den Bosch, S.; Koelewijn, S.-F.; Beckham, G. T.; Sels, B. F. Chemicals from Lignin: An Interplay of Lignocellulose Fractionation, Depolymerisation, and Upgrading. *Chem. Soc. Rev.* **2018**, *47* (3), 852−908.
(6) Crestini, C.; Lange, H.; Sette, M.; Argyropoulos, D. S. On the Structure of Softwood Kraft Lignin. *Green Chem.* **2017**, *19* (17), 4104−4121.
(7) Schulze, P.; Leschinsky, M.; Seidel-Morgenstern, A.; Lorenz, H. Continuous Separation of Lignin from Organosolv Pulping Liquors: Combined Lignin Particle Formation and Solvent Recovery. *Ind. Eng. Chem. Res.* **2019**, *58* (9), 3797−3810.
(8) Yoo, C. G.; Li, M.; Meng, X.; Pu, Y.; Ragauskas, A. J. Effects of Organosolv and Ammonia Pretreatments on Lignin Properties and Its Inhibition for Enzymatic Hydrolysis. *Green Chem.* **2017**, *19* (8), 2006−2016.
(9) Zijlstra, D. S.; Analbers, C. A.; de Korte, J.; Wilbers, E.; Deuss, P. J. Efficient Mild Organosolv Lignin Extraction in a Flow-Through Setup Yielding Lignin with High β-O-4 Content. *Polymers* **2019**, *11* (12), 1913.
(10) Azadi, P.; Inderwildi, O. R.; Farnood, R.; King, D. A. Liquid Fuels, Hydrogen and Chemicals from Lignin: A Critical Review. *Renewable Sustainable Energy Rev.* **2013**, *21*, 506−523.
(11) Laurichesse, S.; Avérous, L. Chemical Modification of Lignins: Towards Biobased Polymers. *Prog. Polym. Sci.* **2014**, *39* (7), 1266−1290.
(12) Li, C.; Zhao, X.; Wang, A.; Huber, G. W.; Zhang, T. Catalytic Transformation of Lignin for the Production of Chemicals and Fuels. *Chem. Rev.* **2015**, *115* (21), 11559−11624.
(13) Kai, D.; Tan, M. J.; Chee, P. L.; Chua, Y. K.; Yap, Y. L.; Loh, X. J. Towards Lignin-Based Functional Materials in a Sustainable World. *Green Chem.* **2016**, *18* (5), 1175−1200.
(14) Crestini, C.; Melone, F.; Sette, M.; Saladino, R. Milled Wood Lignin: A Linear Oligomer. *Biomacromolecules* **2011**, *12* (11), 3928−3935.
(15) Vanholme, R.; Demedts, B.; Morreel, K.; Ralph, J.; Boerjan, W. Lignin Biosynthesis and Structure. *Plant Physiol.* **2010**, *153* (3), 895−905.
(16) Thoresen, P. P.; Matsakas, L.; Rova, U.; Christakopoulos, P. Recent Advances in Organosolv Fractionation: Towards Biomass Fractionation Technology of the Future. *Bioresour. Technol.* **2020**, *306*, 123189.
(17) Weidener, D.; Leitner, W.; Domínguez de María, P.; Klose, H.; Grande, P. M. Lignocellulose Fractionation Using Recyclable Phosphoric Acid: Lignin, Cellulose, and Furfural Production. *ChemSusChem* **2021**, *14* (3), 909−916.
(18) Weidener, D.; Klose, H.; Leitner, W.; Schurr, U.; Usadel, B.; Domínguez de María, P.; Grande, P. M. One-Step Lignocellulose Fractionation by Using 2,5-Furandicarboxylic Acid as a Biogenic and Recyclable Catalyst. *ChemSusChem* **2018**, *11* (13), 2051−2056.
(19) Grande, P. M.; Viell, J.; Theyssen, N.; Marquardt, W.; Domínguez de María, P.; Leitner, W. Fractionation of Lignocellulosic Biomass Using the OrganoCat Process. *Green Chem.* **2015**, *17* (6), 3533−3539.
(20) Weidener, D.; Dama, M.; Dietrich, S. K.; Ohrem, B.; Pauly, M.; Leitner, W.; Domínguez de María, P.; Grande, P. M.; Klose, H. Multiscale Analysis of Lignocellulose Recalcitrance towards Organo-Cat Pretreatment and Fractionation. *Biotechnol. Biofuels* **2020**, *13* (1), 155.
(21) Damm, T.; Grande, P. M.; Jablonowski, N. D.; Thiele, B.; Disko, U.; Mann, U.; Schurr, U.; Leitner, W.; Usadel, B.; Domínguez de María, P.; Klose, H. OrganoCat Pretreatment of Perennial Plants: Synergies between a Biogenic Fractionation and Valuable Feedstocks. *Bioresour. Technol.* **2017**, *244*, 889−896.
(22) Foster, C. E.; Martin, T. M.; Pauly, M. Comprehensive Compositional Analysis of Plant Cell Walls (Lignocellulosic Biomass) Part I: Lignin. *J. Vis. Exp.* **2010**, *37*, 5−8.
(23) Foster, C. E.; Martin, T. M.; Pauly, M. Comprehensive Compositional Analysis of Plant Cell Walls (Lignocellulosic Biomass) Part II: Carbohydrates. *J. Vis. Exp.* **2010**, *37*, 10−13.
(24) Damm, T.; Grande, P. M.; Jablonowski, N. D.; Thiele, B.; Disko, U.; Mann, U.; Schurr, U.; Leitner, W.; Usadel, B.; Domínguez de María, P.; Klose, H. OrganoCat Pretreatment of Perennial Plants: Synergies between a Biogenic Fractionation and Valuable Feedstocks. *Bioresour. Technol.* **2017**, *244*, 889−896.
(25) Cheng, K.; Sorek, H.; Zimmermann, H.; Wemmer, D. E.; Pauly, M. Solution-State 2D NMR Spectroscopy of Plant Cell Walls Enabled by a Dimethylsulfoxide- d_6/1-Ethyl-3-Methylimidazolium Acetate Solvent. *Anal. Chem.* **2013**, *85* (6), 3213−3221.
(26) Hatfield, R. D.; Jung, H.-J. G.; Ralph, J.; Buxton, D. R.; Weimer, P. J. A Comparison of the Insoluble Residues Produced by the Klason Lignin and Acid Detergent Lignin Procedures. *J. Sci. Food Agric.* **1994**, *65* (1), 51−58.
(27) Kishimoto, T.; Chiba, W.; Saito, K.; Fukushima, K.; Uraki, Y.; Ubukata, M. Influence of Syringyl to Guaiacyl Ratio on the Structure of Natural and Synthetic Lignins. *J. Agric. Food Chem.* **2010**, *58* (2), 895−901.
(28) Vermaas, J. V.; Crowley, M. F.; Beckham, G. T. Molecular Lignin Solubility and Structure in Organic Solvents. *ACS Sustain. Chem. Eng.* **2020**, *8* (48), 17839−17850.
(29) Vural, D.; Smith, J. C.; Petridis, L. Polymer Principles behind Solubilizing Lignin with Organic Cosolvents for Bioenergy. *Green Chem.* **2020**, *22* (13), 4331−4340.
(30) Ralph, J.; Lapierre, C.; Boerjan, W. Lignin Structure and Its Engineering. *Curr. Opin. Biotechnol.* **2019**, *56*, 240−249.
(31) Kim, H.; Padmakshan, D.; Li, Y.; Rencoret, J.; Hatfield, R. D.; Ralph, J. Characterization and Elimination of Undesirable Protein Residues in Plant Cell Wall Materials for Enhancing Lignin Analysis by Solution-State Nuclear Magnetic Resonance Spectroscopy. *Biomacromolecules* **2017**, *18* (12), 4184−4195.
(32) Zhang, T.; Zhang, S.; Lan, W.; Yue, F. Quantitative Extraction of P-Coumaric Acid and Ferulic Acid in Different Gramineous Materials and Structural Changes of Residual Alkali Lignin. *J. Renewable Mater.* **2023**, *11* (2), 555−566.
(33) Happs, R. M.; Addison, B.; Doeppke, C.; Donohoe, B. S.; Davis, M. F.; Harman-Ware, A. E. Comparison of Methodologies Used to Determine Aromatic Lignin Unit Ratios in Lignocellulosic Biomass. *Biotechnol. Biofuels* **2021**, *14* (1), 58.
(34) Shen, Q.; Fu, Z.; Li, R.; Wu, Y. A study on the pyrolysis mechanism of a β-O-4 lignin dimer model compound using DFT combined with Py-GC/MS. *J. Therm. Anal. Calorim.* **2021**, *146* (4), 1751−1761.
(35) Happs, R. M.; Addison, B.; Doeppke, C.; Donohoe, B. S.; Davis, M. F.; Harman-Ware, A. E. Comparison of Methodologies Used to Determine Aromatic Lignin Unit Ratios in Lignocellulosic Biomass. *Biotechnol Biofuels* **2021**, *14* (1), 58.
(36) Ohra-Aho, T.; Gomes, F. J. B.; Colodette, J. L.; Tamminen, T. S/G Ratio and Lignin Structure among Eucalyptus Hybrids Determined by Py-GC/MS and Nitrobenzene Oxidation. *J. Anal. Appl. Pyrolysis* **2013**, *101*, 166−171.
(37) Gardner, D. J.; Schultz, T. P.; Mcginnis, G. D. The Pyrolytic Behavior of Selected Lignin Preparations. *J. Wood Chem. Technol.* **1985**, *5* (1), 85−110.
(38) del Río, J. C.; Gutiérrez, A.; Hernando, M.; Landín, P.; Romero, J.; Martínez, T. Determining the Influence of Eucalypt Lignin Composition in Paper Pulp Yield Using Py-GC/MS. *J. Anal. Appl. Pyrolysis* **2005**, *74*, 110.
(39) del Río, J.; Gutiérrez, A.; Romero, J.; Martínez, M.; Martínez, A. Identification of Residual Lignin Markers in Eucalypt Kraft Pulps by Py-GC/MS. *J. Anal. Appl. Pyrolysis* **2001**, *58*−*59*, 425−439.
(40) Kuroda, K.-I. Analytical Pyrolysis Products Derived from Cinnamyl Alcohol-End Groups in Lignins. *J. Anal. Appl. Pyrolysis* **2000**, *53*, 123−134.

https://doi.org/10.1021/acs.energyfuels.3c03673
Energy Fuels 2024, 38, 4192−4202

(41) Kuroda, K.-I.; Nakagawa-Izumi, A. Analytical Pyrolysis of Lignin: Products Stemming from b-5 Substructures. *Org. Geochem.* **2006**, *37*, 665.
(42) Akazawa, M.; Kojima, Y.; Kato, Y. Effect of pyrolysis temperature on the pyrolytic degradation mechanism of *β*-aryl ether linkages. *J. Anal. Appl. Pyrolysis* **2016**, *118*, 164−174.
(43) Kawamoto, H. Lignin Pyrolysis Reactions. *J. Wood Sci.* **2017**, *63* (2), 117−132.
(44) Kawamoto, H.; Watanabe, T.; Saka, S. Strong Interactions during Lignin Pyrolysis in Wood - A Study by in Situ Probing of the Radical Chain Reactions Using Model Dimers. *J. Anal. Appl. Pyrolysis* **2015**, *113*, 630−637.
(45) Tarasov, D.; Leitch, M.; Fatehi, P. Lignin-Carbohydrate Complexes: Properties, Applications, Analyses, and Methods of Extraction: A Review. *Biotechnol. Biofuels* **2018**, *11* (1), 269.

https://doi.org/10.1021/acs.energyfuels.3c03673
Energy Fuels 2024, 38, 4192−4202